COMPARISON OF N-HETEROCYCLIC AMINE LIGANDS FOR POTENTIAL APPLICATION AS ALZHEIMER'S DISEASE THERAPUETIC AGENTS

by

Madalyn M. Barnett

Submitted in partial fulfillment of the

requirements for Departmental Honors in

the Department of Chemistry and Biochemistry

Texas Christian University

Fort Worth, Texas

May 6th, 2019

COMPARISON OF N-HETEROCYCLIC AMINE LIGANDS FOR POTENTIAL APPLICATION AS ALZHEIMER'S DISEASE THERAPUETIC AGENTS

Project Approved:

Supervising Professor: Kayla N. Green, Ph.D.

Department of Chemistry & Biochemistry

Benjamin Sherman, Ph.D.

Department of Chemistry & Biochemistry

Giridhar Akkaraju, Ph.D.

Department of Biology

ABSTRACT

Alzheimer's Disease (AD) has a complex pathology that involves many potential players including, reactive oxygen species (ROS), mis-regulated metal ions, protein aggregations, and cholinergic signaling defects. Thus, many potential therapeutics being investigated are designed to target more than just one of these pathological components. However, to date, there has yet to be any approved drugs that effectively and safely cure or prevent the onset of AD. Green and co-workers have taken this multi-target directed ligand approach by designing and synthesizing metal chelating molecules that contain antioxidant and radical scavenging moieties. The idea behind this approach is that we can target mis-regulated metal ions and decrease ROS while also potentially effecting other players of AD pathology. To test and compare the potential application of the newly synthesized **L4** to previously synthesized **L2**, various spectroscopic assays were utilized. These assays specifically looked at the ability to inhibit amyloid aggregation (a hallmark observed in AD patients), inhibit ROS production via redox cycling, and scavenge radical species. Results from the aggregation inhibition study were unexpected due to ligand-metal complex solubility within the assay conditions. **L4** did show it could effectively prevent ROS production, primarily thanks to its stable metal binding conformation. Lastly, results from one of the radical scavenging assays showed increased potential of **L4** compared to **L2** to act as a radical scavenger while the second assay did not give the same results as expected but this was hypothesized to be due to reaction parameters. Overall, these finding still support the potential of **L4** to act as a therapeutic agent for AD, but other modifications or studies must be performed for further validation.

ACKNOWLDGEMENTS

I would like to sincerely thank everyone who made this thesis project possible, including my committee, the John V. Roach Honors College, the College of Science and Engineering, and the Chemistry & Biochemistry Department. This experience will forever be an important part of my undergraduate story.

First and foremost, I must specifically thank Dr. Green for her unwavering support and confidence in me from the start. She welcomed me into her lab as a bright-eyed sophomore and, even then, believed I could be very successful. Thank you, Dr. Green, for being a great mentor during my time here at TCU, both in the lab and through my involvement with the TCU chemistry club. I know you will continue to inspire more students with your passion, sincerity, and understanding.

To the undergraduate Green Group members who have come before me, thank you for showing me the way and welcoming me into your team. To those undergraduate members who have followed in my path, thank you for keeping me humble and reminding me I still have so much more to learn. I have enjoyed working and learning alongside each of you and look forward to hearing about all that you will accomplish. A big thank you to Brian for driving me crazy while keeping me sane all at the same time. I am so glad I had you by my side during this long, sometimes weird, journey. Thank you to Tim for all that you have done and continue to do as well! Your passion for this lab and science has always served as a great reminder for why I was here.

I must especially thank the graduate students who welcomed me into the lab and were always there to answer questions, give advice, and of course, show that science could be fun. Hannah, thank you for all your contributions that made this project possible. Without you, there would be no **L4**. Samantha, thank you for always being in the lab so that I could continue working at weird hours. And of course, thank you Marianne. You not only quite literally helped me on every step of this project, but also became one of my best friends and continue to inspire me every day. The stories we have from our time in the Green group could fill a book, and I would never get tired of reading said book. To say we were basically the same person would be an understatement, and I have never been happier to be a member of the MB club.

TABLE OF CONTENTS

LIST OF FIGURES

Figure 6. DPPH assay showing the radical scavenging abilities of **L2** and **L4** as compared to the positive controls BHT and ascorbic acid. 17

LIST OF TABLES

LIST OF SCHEMES

INTRODUCTION

I. Alzheimer's Disease: Impact and Pathology

The neurodegenerative disorder Alzheimer's disease (AD) is the most prevalent form of dementia and accounts for 60-80% of cases.[1] According to the Alzheimer's Association report, an estimated 5.7 million Americans were living with AD in 2018,[2] and that by 2050, someone will develop Alzheimer's dementia every 33 seconds.[1-2] Unfortunately, there is currently no cure and only a select, few drugs have been approved by the FDA to help manage some of the symptoms associated with AD.[3] Thus, AD is listed as the sixth-leading cause of death in the United States.[2] To make matters worse, the financial and emotional toll this disease has on patients and their families is daunting. For example, the estimated total lifetime cost of care for someone with dementia as of 2017 was $332,399.[4]

Perhaps the most well-identified aspects of AD are the common symptoms manifested over time, including a decline in language and motor skills, sensory information processing, and, of course, memory formation and retrieval.[5] In contrast to this, the primary pathology hallmarks and cause of AD continue to be a major debate amongst researchers. There have been several pathological hypotheses developed in pursuit of elucidating the primary causative factors of AD including: (i) amyloid cascade hypothesis; (ii) tau hypothesis; (iii) metal ion cascade hypothesis; (iv) oxidative stress hypothesis; and (v) cholinergic hypothesis (Table 1).[3] The work presented in this thesis focuses on targeting aspects related to hypotheses (i), (iii), and (iv) because of their apparent overlap and will be discussed in further detail herein.

Table 1. Examples of contributing pathological hypotheses for Alzheimer's disease.

Entry	Hypothesis	Pathology observed
(i)	Amyloid Cascade	Senile plaques (SP) and toxic oligomers composed of amyloid-β (Aβ) aggregates are causative factor of AD.[3, 6-7]
(ii)	Tau	Neurofibrillary tangles (NFTs) composed of hyperphosphorylated tau proteins (ptua) correlate closely with neurodegredation.[3, 6, 8-9]
(iii)	Metal Ion Cascade	Metal ions (primarily Cu, Fe, and Zn) contribute to AD pathology via dyshomeostasis and mis-compartmentalization.[3, 10-11]
(iv)	Oxidative Stress	The cellular damage initiated by reactive oxygen species (ROS) can contribute to multiple pathogenic pathways of AD.[3, 10, 12-13]
(v)	Cholinergic	The degradation of cholinergic neurons and associated cholinergic neurotransmitters contribute the cognitive function deterioration seen in brains of AD patients.[3, 14-15]

II. Amyloid, Oxidative Stress, and Metal-ion Integrated Pathology of AD

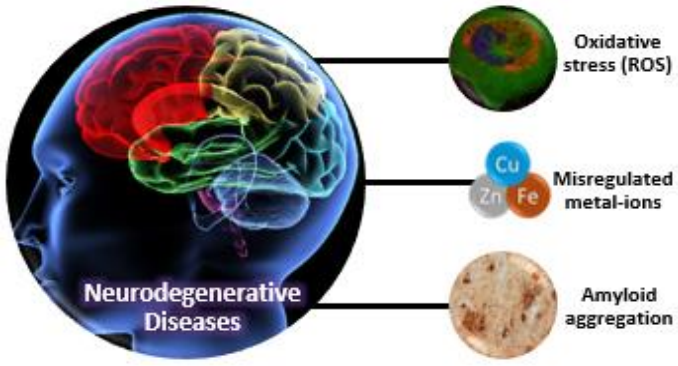

Figure 1. The pathological trifecta of Alzheimer's Disease.[16]

According to the amyloid cascade hypothesis, the cause of AD is an imbalance between Aβ production and clearance and the main neurotoxic element is the aggregates.[12] The metal ion

cascade hypothesis states that AD and the Aβ imbalance is primarily a consequence of impaired metal homeostasis.[12] Lastly, the oxidative stress hypothesis states that the gene defects and mitochondrial function decline that result from enhanced oxidative stress due to reactive oxygen species (ROS) leads to the neurological decline observed in patients with AD.[12] While there is evidence that supports each of these hypotheses, there are also indications that these hypotheses come together to form a pathological trifecta for AD (Figure 1).[16] It is important to first note that Aβ, metal ions, and ROS all have a role in normal, healthy functioning individuals, thus homeostasis disruption is a major theme in this pathology trifecta.

Aβ is an innate protein found within the brain and is derived from cleavage of the amyloid precursor protein (APP) by protease and secretase enzymes.[12, 17-18] Of the two cleavage pathways that APP undergoes; the amyloidogenic pathway specifically results in the formation of $A\beta_{40}$ and $A\beta_{42}$.[12] These two Aβ peptides are found in various forms including the toxic soluble oligomers, protofibrils, and the insoluble extracellular aggregates or senile plaques (SP).[12, 19] Any imbalance between the pathways or clearance of the Aβ products can contribute to their accumulation and subsequent pathological effects observed in AD patients.

Metal ions, specifically those of Cu, Fe, and Zn, are necessary for many internal biological systems, including that of the Aβ pathway.[12, 19] They are also essential for many neuronal functions including oxygen transport, electron transport, neurotransmitter synthesis, and free radical detoxification.[20-21] If concentrations of these metal ions are not tightly regulated, problems arise in these pathways and many other secondary effects occur. It has been shown

that increases in the free metal ion concentrations can lead to protein aggregation (as seen with the Aβ peptides) and oxidative stress.[16, 22] Evidence of Aβ plaques that contain increased amounts of Cu(II), Zn(II), and Fe(III) are also consistent with the metal-amyloid pathology.[16]

Oxidative stress is the third component of this trifecta and further connects the other two pillars. Oxidative stress is the result of excess reactive oxygen species (ROS), which often are in the form of free radicals, and are natural byproducts of oxidative phosphorylation or aerobic metabolism.[16, 20-21] A few examples include superoxide anion ($O_2^{-\bullet}$), hydroxyl radical ($OH^{\bullet}$), and hydrogen superoxide ($HO_2^{\bullet}$).[21, 23] ROS induce damaging effects to lipids, DNA, and proteins during oxidative stress .[10, 16, 20-21, 23] Fenton chemistry is another significant pathway through which ROS are generated utilizing hydrogen peroxide and metal ions.[16, 20-21, 23] As mentioned above, the amyloid plaques themselves also induce ROS production and, when bound to the metal ions, also contribute to the Fenton Chemistry.

III. Approach to Therapeutics

As described previously, there are currently only a handful of FDA approved drugs for managing the symptoms associated with AD. These include four acetylcholinesterase inhibitors (AChEIs)—donepezil, tacarine, rivastigmine, and galantamine—which reportedly improve memory and cognitive function to an extent, but fail to prevent, halt, or reverse the overall progression of AD.[24-25] Many other approaches focus on using metal chelators like Clioquinol (CQ) and cyclen to sequester the mis-regulated metal ions recognized as potential pathogenic instigators.[16, 21] That being said, as more is understood about the complex pathology associated with AD, most research has been directed towards developing multi-target-directed ligands (MTDL) for potential application as therapeutic agents.[25-28] In addition

to functionality and target-specific moieties, other aspects of a potential therapeutic must be considered. These aspects include overall stability, water solubility, gram-scale availability, and biocompatibility in terms of toxicity and blood-brain-barrier (BBB) permeability.

IV. A multimodal approach by Green and co-workers

The MTDL approach is currently being explored by the Green Group through the synthesis and investigation of the therapeutic applications of a library of metal-binding azamacrocycles (Figure 2).[16, 18, 21, 29] Green and co-workers developed this library to primarily target the overlapping factors associated with the Aβ aggregation, mis-regulated metal ions, and ROS as discussed above. The pyridine- and pyridol-based ligand library initially expanded on the work of Stetter and coworkers who first reported pyclen (**L1**) in 1981.[16] **L1** showed the ability to chelate Cu^{2+}, Fe^{3+}, and Zn^{2+} (biologically relevant metals).[20-21, 29] **L1** also acts as an antioxidant as a result of N-oxide formation within the conjugated pyridine ring.[20-21, 29] Lastly, studies showed that **L1** could inhibit and disaggregate metal-induced Aβ plaques.[29]

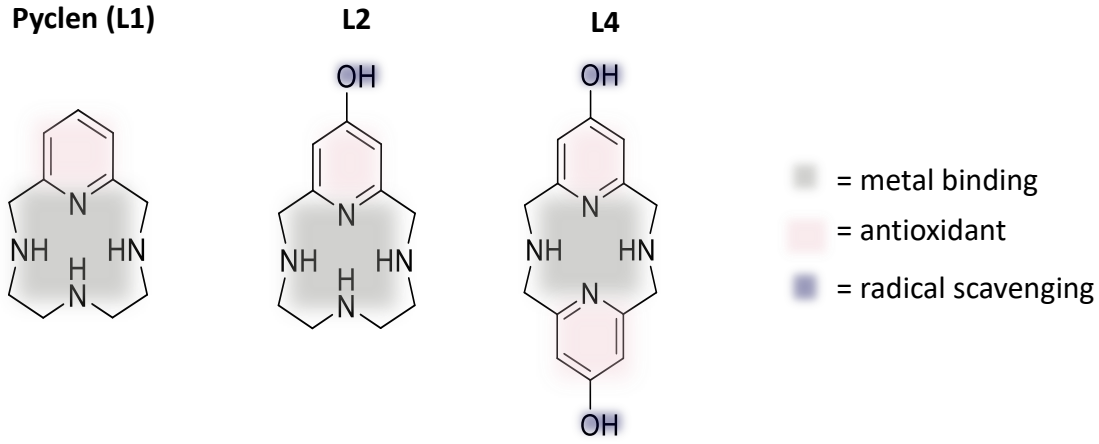

Figure 2. Green Group ligand library and functional assignments.

L2 was designed based on the hypothesis that adding an electron donating (ED) functional group such as -OH in the *para* position of the pyridine ring would increase the antioxidant

capabilities without affecting the other functionalities of **L1**. Results from several biological assays evaluating the antioxidant and radical scavenging character of **L2** showed increased radical scavenging and antioxidant abilities compared to **L1**.[20] **L2** also maintained the metal-chelating properties of **L1**.[30]

With the relative success of the radical scavenger and pyridol-based **L2** compared to **L1**, it was hypothesized that by doubling the number of pyridol moieties to form **L4**, the therapeutic effect could be enhanced further. This would theoretically increase the radical scavenging and antioxidant capabilities while simultaneously increasing the potency. Testing this hypothesis was one of the main goals of this project and involved using several relevant assays, including the Coumarin-3-carboxylic acid (CCA) redox cycling assay, 2,2-diphenyl-1-picrylhydrazyl (DPPH) radical quenching assay, and Trolox equivalency antioxidant capacity (TEAC) assay, to compare **L2** and **L4** along with other antioxidant standards. Along with these studies, the ability of **L4** to inhibit or induce disaggregation of Aβ will be evaluated using a turbidity and thioflavin T assay. To begin, I will discuss briefly the synthesis and metalation results obtained by other members of the group and will then describe the results of the assays performed to evaluate the potential application of **L4** as an AD therapeutic.

MATERIALS AND METHODS

I. General synthesis

The synthesis of **L4**, as completed and reported by Hannah Johnston[31] and based on work published in Bottino *et al*.[32-35] was achieved in a 1:1 condensation reaction shown in Scheme 1. Two equivalents of tosylamide monosodium (TsNHNa) were combined with **1** (4-benzyloxy-2,6-bis(chloromethyl)pyridine in DMF under reflux to produce the cyclized and tosyl-protected product **2**.[16, 36] This cyclization reaction can be visualized as proceeding through a monoalkylated-intermediate followed by self-condensation in the presence of excess TsNHNa, which acts as a base, to yield the desired macrocyclic product (Scheme S1).[16, 36] The solid-state structure of **2** obtained through X-ray diffraction analysis is observed in the lowest energy *syn* confirmation. The removal of both the benzyl and tosyl protecting groups from **2** is accomplished in one-step with a naphthalene-catalyzed lithiation reaction (Scheme 1).[16, 37-38] The reaction mixture is then hydrolyzed and an acid work-up yields **L4** as the trihydrochloride salt. NMR analysis was consistent with the connectivity shown in Scheme 1. The ligand is highly soluble in water but only soluble in polar organic solvents in the basic form.

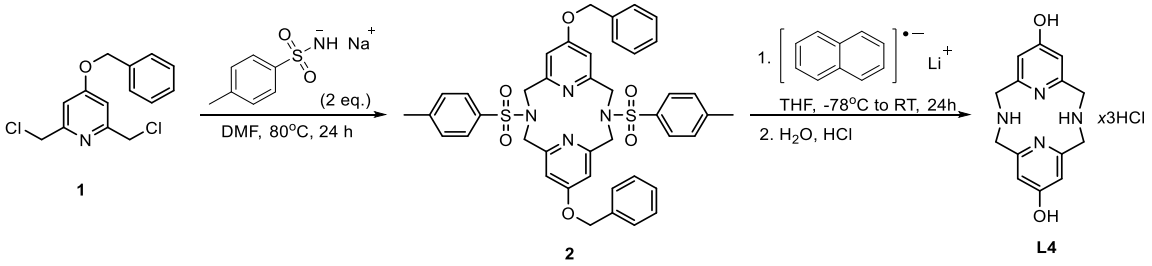

Scheme 1. Synthetic methodology for the isolation of **L4.**

II. Metalation

The complexation reactions were carried out by co-worker Hannah Johnston.[31] Molecule **L4** (42.5 mg, 0.123 mmol) was weighed out and dissolved in 5 mL of water to give a clear-light yellow solution. The pH of the ligand solution was adjusted to 5.5 using a 1.0 M solution of KOH. $Cu(ClO_4)_2 \bullet 6\ H_2O$ (45.6 mg, 0.123 mmol) was subsequently weighed out and dissolved in 1 mL of H_2O. The metal solution was slowly added dropwise to the pH adjusted ligand solution to initiate the metalation. Immediately the solution color changed from light yellow to light blue; this solution was stirred at room temperature, open to air, for 24 h. The reaction mixture was subsequently evaporated under reduced pressure to afford a light green solid. The solid was dissolved in a minimum amount of CH_3OH (1 mL) and a very small amount of H_2O was added (0.8 mL). Any remaining salts left undissolved were filtered out of the solution; the filtered solution was set out for crystal growth. After several days more salts crashed out of solution, these were subsequently removed by filtration and the solutions were set out for slow evaporation crystallization again. After several cycles of filtering the solution and setting it out for slow evaporation, light green X-ray quality crystals of **CuL4** were isolated (15.1 mg, 0.017 mmol, 28% yield). Electronic absorption, λ_{max}/nm ($\varepsilon/M^{-1}\ cm^{-1}$); H_2O: 758 (23); DMF: 873 (49). ESI-MS$^+$ Calc (Found), $[M]^+$: *m/z*= 370.0258 (369.8742). [31]

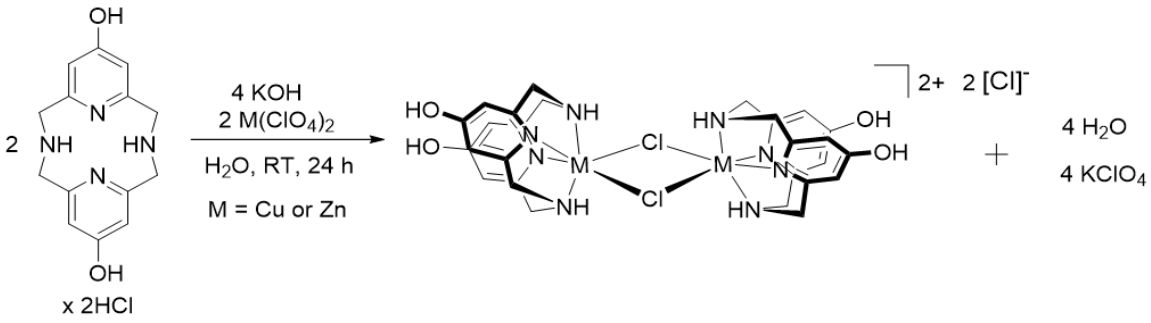

Scheme 2. Complexation reaction of **L4** with Cu(II) and Zn(II). The $KClO_4$ salts were removed by several cycles of slow evaporation and filtration in MeOH.

III. Turbidity Assay

Turbidity inhibition studies were carried out using amyloid, copper(II), and metal chelators to determine the ability of **L4** to prevent amyloid aggregation as compared to **L2** and cyclen. The amyloid $\beta_{1\text{-}40}$ was dissolved in NH_4OH (1% v/v aq) to prepare a ~200 µM solution. The Cu(II) stock solution (1 mM) was prepared by dissolving $CuCl_2$ in 10 mL of chelex-treated HEPES buffer (pH 6.6) and then diluted with buffer to prepare a 0.4 mM solution. Cyclen, **L2**, and **L4** solutions (0.8 mM) were also all prepared in chelex-treated HEPES buffer (pH 6.6). These stock solutions were then used to prepare samples of various combinations of the three components and diluted with HEPES buffer so that the final concentrations were 20 µM (amyloid), 40 µM (Cu), and 80 µM (ligand). Tyrosine fluorescence was then used to quantify aggregation. For sample preparation, 100 µL of each sample was diluted with 200 µL of buffer in a 300 µL single-cell cuvette. Excitation and emission values utilized were 278 nm and 308 nm, respectively.

IV. CCA Assay

All stock solutions were prepared separately in PBS buffer (1X, pH 7.4) except $CuSO_4 \cdot 6H_2O$, which was dissolved and diluted in Milli-Q water. Final sample volume = 3 mL. Each experiment was performed in triplicate (n = 3). Hydroxyl radical production was followed by measuring the conversion of CCA into 7-hydroxy-CCA (λ_{ex} = 395 nm, λ_{em} = 450 nm). General order of addition: PBS buffer (2200 µL for positive control, 2150 µL for 0.5 eq. samples, 2100 µL for 1 eq. samples, 2300 µL for neg controls), CCA [100 µM, 500 µL], Desferal [1 µM, 100 µL], molecule **L2** or **L4** [½ eq. = 5 µM, 50 µL; 1 eq. = 10 µM, 100 µL], Cu(II) [10 µM, 100 µL], then ascorbate [300 µM, 100 µL].

V. DPPH assay

A stock solution of the DPPH radical was prepared by dissolving 17.8 mg in 300 mL of methanol (150 µM). A solid sample of **L4**, ascorbic acid, or butylated hydroxytoluene (BHT) were dissolved in 10 mL methanol (stock concentration 5 mM). A solid sample of **L2** was dissolved in 10 mL of water and the pH was adjusted to 7 using 1.0 M KOH. The water was then removed using the rotovap and the sample was dissolved in 10 mL of methanol (stock concentration 5 mM). Next, the sample solutions were prepared in 7 mL-vials by diluting the stock solutions (5 mM) with methanol to various concentration (2-3000 µM, 1 mL). Next, each working sample was prepared by mixing 100 µL of one of the prepared samples with 100 µL of the DPPH stock directly in the 96-well plate to final concentrations ranging from 1-1500 µM. A separate well plate was used for each sample and each concentration was analyzed in triplicate. An aliquot of the DPPH stock solution (100 µL) was mixed with methanol (100 µL) and was used as a negative control for each sample. The samples were incubated in the dark for 30 minutes (as well as 1 hour for **L2** and **L4)**, at room temperature. For analysis, each well plate was run using the BMG Labtech FLUOstar Omega UV/Vis absorbance spectrophotometer microplate reader. The absorbance at 516 nm of each sample was measured. Each experiment was performed in triplicate (n = 3). The final absorbance values have been normalized to the average (n = 3) absorbance of the negative control DPPH sample and are expressed as the % DPPH radical quenched.

VI. TEAC assay

The TEAC assay was a second method used to test the radical scavenging ability of the representative compounds compared to additional antioxidant standards such as α-

tocopherol (α-toc) and ascorbic acid (asc. acid). Trolox (6-hydroxy-2,5,7,8-tetramethylchroman-2-carboxylic acid) itself is an α-tocopherol analog. To produce the $ABTS^{\bullet+}$ (2,2'-azinobis-(3-ethylbenzothiazoline-6-sulfonic acid) diammonium salt), ABTS was dissolved in 10 mL of water (7 mM) and then reacted with 2.45 mM potassium persulfate (6.6 mg). This solution was then incubated in the dark for 22 hours at room temperature. Next the $ABTS^{\bullet+}$ was diluted with methanol to an absorbance of approximately 0.7±0.2 at 745 nm (final concentration = 87.5 μM). The Trolox, ascorbic acid, and α-tocopherol solutions were prepared by diluting the compounds in 10 mL of methanol (3 mM) and then diluted with methanol to a working stock of 218.17 μM. Varying concentration samples were then prepared using serial dilutions. The **L2** and **L4** solutions were prepared by diluting the compounds the 6 mL of DI-water, adjusting the pH to 7.0, removing the solvent, and then dissolving in 6 mL of methanol (6 mM). This stock was used to prepare samples of varying concentrations for analysis. For the absorbance measurements, 0.5 mL of the sample was mixed with 2.5 mL of $ABTS^{\bullet+}$ in a 3 mL cuvette and the absorbance was measured at 745 nm. Each sample data set was plotted to obtain a linear system of concentration vs. absorbance. The slope of each was normalized with respect to the Trolox in order to obtain the TEAC value.

RESULTS AND DISCUSSION

I. Turbidity assay

The turbidity assay is a method that allows us to determine if our ligand is capable of facilitating the disaggregation of β-amyloid. Aggregation is facilitated by the presence of metal-ions.[39-42] It goes through a series of oligomers and then plaque aggregation. Therefore, the following experiments were designed to test if the molecules of interest can bind the copper and prevent this aggregation. In this assay, amyloid$_{1\text{-}40}$ aggregation is initiated by the addition of transition metal solutions to amyloid as well as the metal binding compound. Fluorescence spectroscopy was used to evaluate the levels of aggregation compared to controls where no metal binding compound was added. Non-aggregated amyloid has natural fluorescence thanks to the tyrosine in position 10 of the peptide chain.[43-45] As shown in Figure 3, non-aggregated amyloid shows an intense fluorescence signal at 308 nm when irradiated at 278 nm. A significant decrease in fluorescent signal is observed when Cu(II) is added due to the amyloid aggregation and prevention of the Tyrosine-10 rotation, which is responsible for the fluorescent response. Cyclen addition results in a fluorescence signal relatively equal to the non-aggregated amyloid, thus indicating that cyclen is capable of inhibiting aggregation formation by chelating copper. **L2** showed the same inhibiting capabilities of cyclen. However, when **L4** was added into solution with copper an increase in fluorescence units was not observed. This was unexpected and, therefore, explored more closely.

When considering the conditions of this assay, specifically the pH parameters, we hypothesized that the **CuL4** complex is interfering with the fluorescent signal used to monitor amyloid aggregation. So potentiometric titrations of **L4** with copper were carried out at a range of pH value to understand the metal-ligand stability and interaction. Results showed

that at neutral pH the **CuL4** complex precipitates out of solution. This precipitate would explain the decrease in fluorescent units observed. Electron microscopy would be the next step in looking at fibril formation.

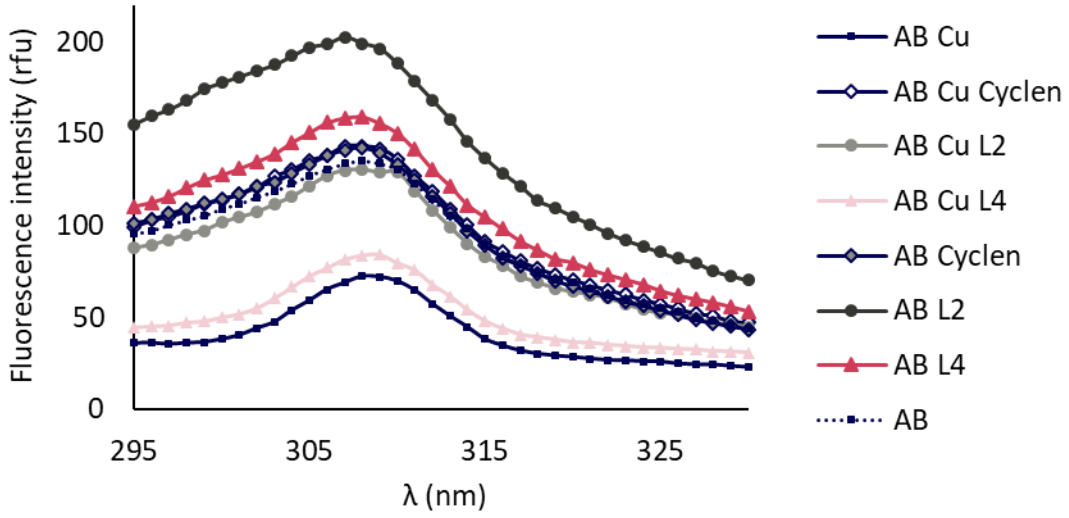

Figure 3. Tyrosine Fluorescence of β-amyloid with various exposure to either metal, ligand, or both. (Excitation wavelength = 278 nm)

II. CCA assay

As discussed previously, one of the contributing factors to the development of AD is the production of ROS. One way this occurs is through the redox cycling of transition metals like copper. A popular model for this process, which can occur in the brain, is the Cu-ascorbate redox system that results in the generation of hydroxyl radicals (Scheme 3). This reaction can be evaluated using the coumarin-carboxylic acid (CCA) assay. As the hydroxyl radicals are produced, they react stoichiometrically with the CCA to form the fluorescent 7-hydroxy-CCA (Scheme 3). The relative fluorescence levels can therefore be used to evaluate and compare the capacity of **L4** and **L2** to halt the metal redox cycling by coordinating with the Cu(II) ions.

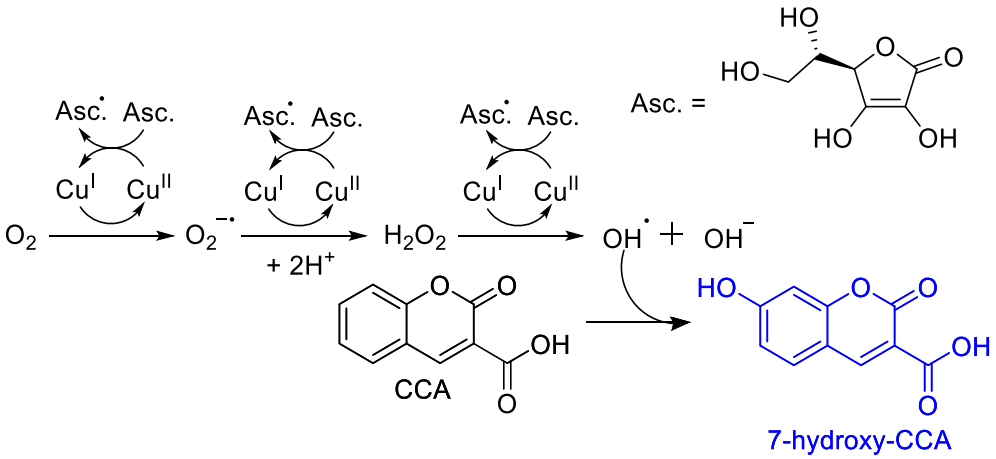

Scheme 3. Cu(II)/Cu(I) redox cycling in the presence of oxygen and ascorbate to produce ROS and the subsequent reaction of the hydroxyl radical with CCA to produce fluorescent 7-hydroxy-CCA.

As shown in Figure 4, the addition of one equivalent of **L2** or **L4** (with respect to Cu(II) concentration) results in almost complete inhibition of 7-hydroxy-CCA fluorescence while the addition of 0.5 equivalent of **L2** or **L4** results in only partial inhibition. The signal observed for the 0.5 equivalent samples is less than 50% of that compared to the positive control. Additionally, data collected from the cyclic voltammetry shows that both **L2** and **L4** shift the Cu(II)/Cu(I) redox cycling to potentials more negative than the redox chemistry of the copper-ascorbate system.[31, 46] The slightly enhanced ability of **L4** to halt redox cycling compared to **L2** can be attributed to the additional pyridol moiety, which may quench hydroxyl radicals that are produced during redox cycling. The ability of **L2** and **L4** to halt the redox cycling of Cu(II) and ascorbate in an aerobic environment makes both of these molecules good

candidates for use as future therapeutic agents to combat the production of excess ROS in the brain.

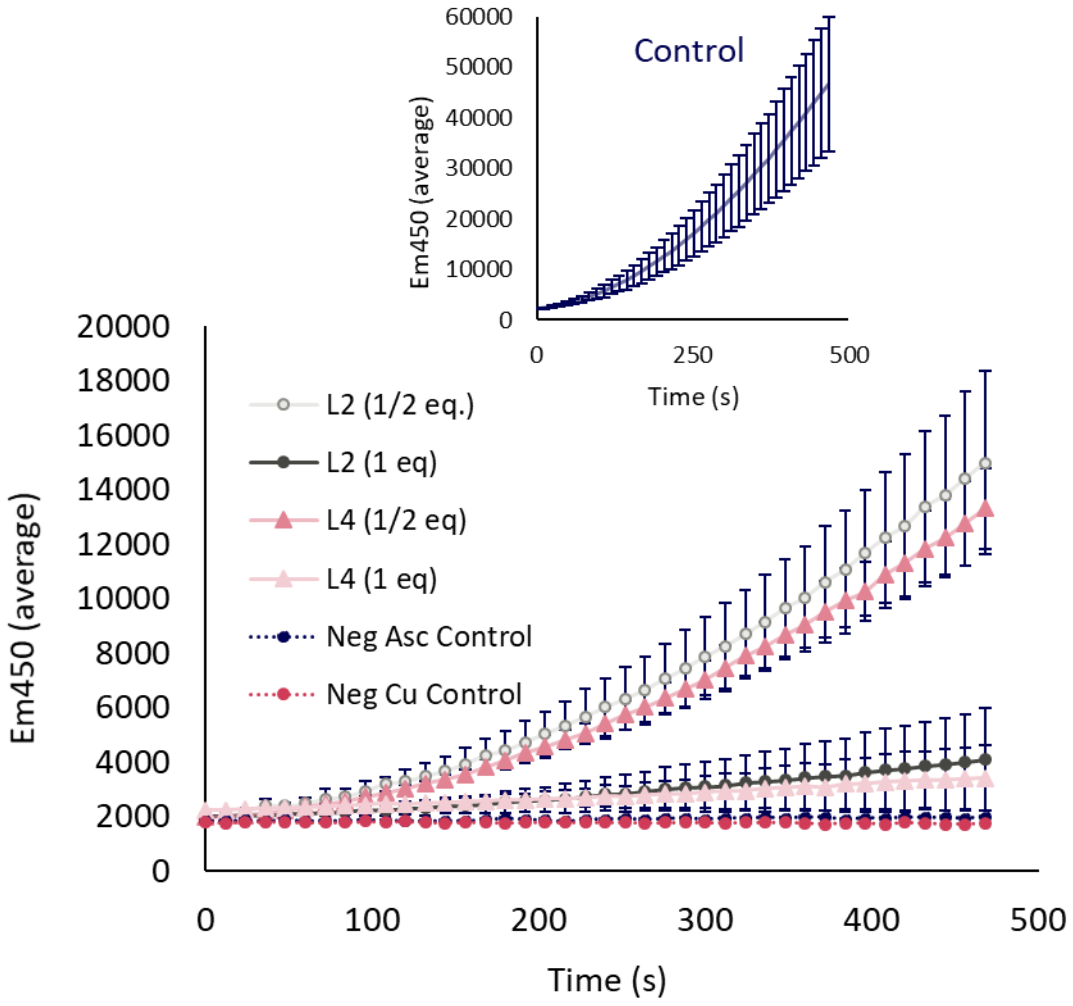

Figure 4. Fluorescence intensity of 7-hydroxy-CCA after incubation of CCA (100 μM) and ascorbate (300 μM) with Cu(II) (10 μM) and either **L2** (1 eq.= 10 μM, 0.5 eq.= 5 μM) or **L4** (1 eq.= 10 μM, 0.5 eq.= 5 μM).

III. DPPH assay

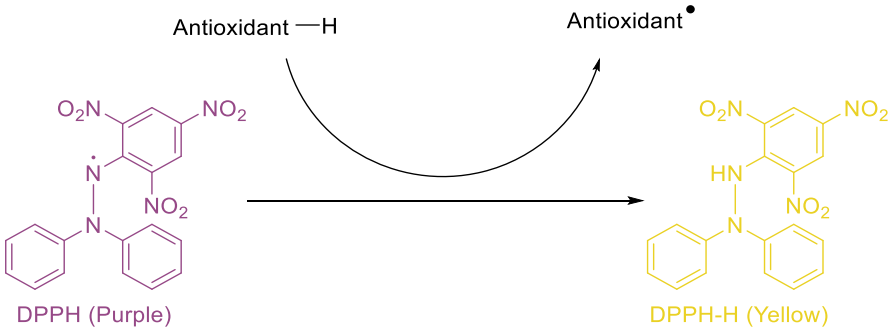

Scheme 4. DPPH antioxidant reaction

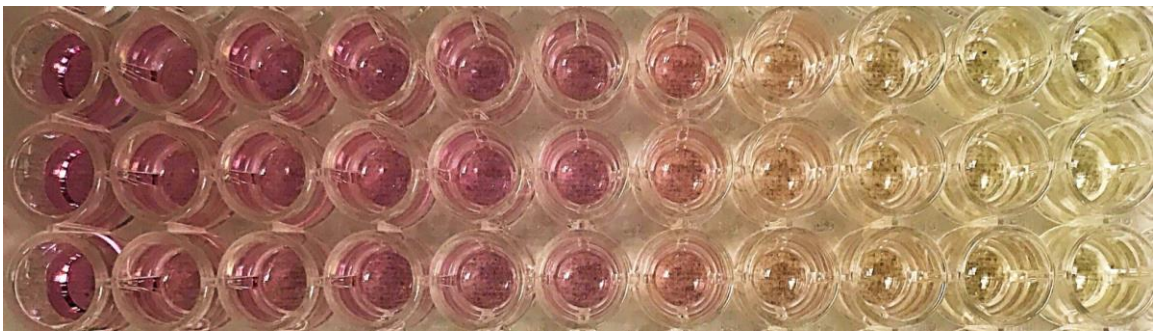

Figure 5. DPPH solution color with increasing antioxidant concentration (left to right).

A first approach used to compare the radical scavenging ability of **L4** to **L2** was the DPPH radical quenching assay. DPPH is a stable radical that is observed to have a maximum absorbance at 515 nm. The DPPH radical is quenched in the presence of a radical scavenging molecule, resulting in a decrease in the absorbance at 515 nm along with a visible color change from a deep purple to pale yellow (Scheme 4, Figure 5). This assay also included two antioxidant positive controls, BHT (butylhydroxytoluene) and ascorbic acid for comparison and the concentrations for each sample ranged from 1 μM to 1500 μM. As shown in Figure 6, the radical scavenging ability of **L4** is about two-fold greater than that of **L2**, and, at higher concentrations, near that of the BHT and ascorbic acid positive controls. These results provide

evidence to support our hypothesis that the doubling of pyridol moieties to form **L4** enhances that radical scavenging and antioxidant abilities as compared to **L2**.

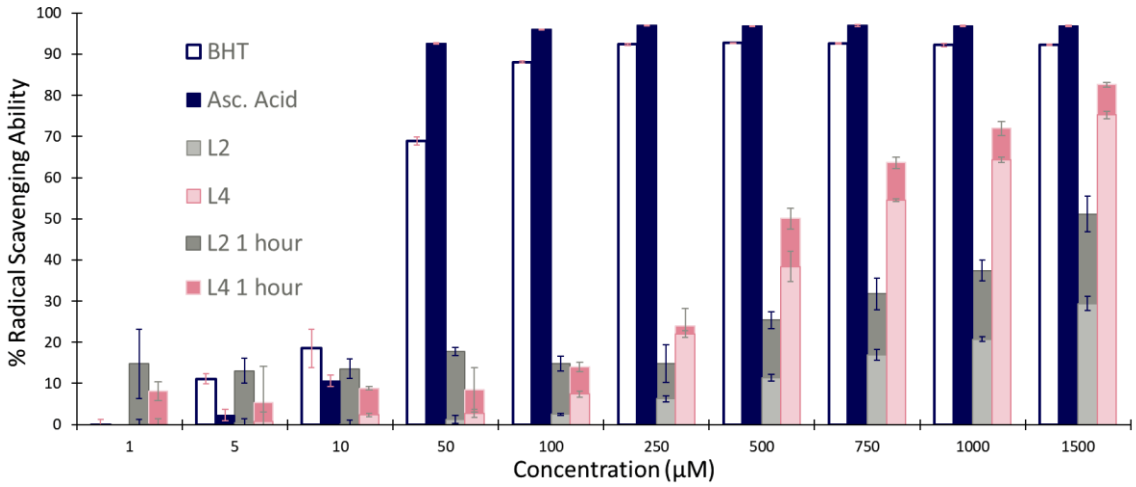

Figure 6. DPPH assay showing the radical scavenging abilities of **L2** and **L4** as compared to the positive controls BHT and ascorbic acid.

IV. TEAC assay

The Trolox equivalent antioxidant capacity (TEAC) assay was a second approach used to compare the radical scavenging ability of **L4** to **L2**. In this assay, Trolox is used as the gold standard antioxidant for the scavenging of the $ABTS^{\bullet+}$ radical cation and α-tocopherol (α-toc) and ascorbic acid (asc. acid) are used for additional comparison. Absorbance spectroscopy was once again used to quantify the radical scavenging abilities of each compound. However, rather than a percentage as with the DPPH assay, the data is reported as the TEAC value. The TEAC value is essentially the radical scavenging ability as compared to the gold standard Trolox. The $ABTS^{\bullet+}$ radical cation absorbs strongly at 745 nm and the reduction in absorbance at this wavelength with the addition of the compounds will give the antioxidant capacity of the compound.[47] **L2** and **L4** both had TEAC values significantly less than α-tocopherol (α-toc)

and ascorbic acid (asc. acid), with **L2** performing slightly better than **L4** (Table 2). These results, though unexpected because of the contradiction to results of the DPPH assay, can be understood by looking at literature comparing the DPPH assay to the TEAC assay. For example, Abramovic and Csepregi reported and described similar contradicting results within their studies.[48-49] This could be due to assay conditions (pH, solvent, solubility, etc.) compound size, or the differences in the mechanism of radical reactions.

Table 2. TEAC values for compounds **L2** and **L4** compared to the positive antioxidant controls α-tocopherol (α-toc) and ascorbic acid (asc. acid).

Compound	TEAC value
trolox	1.0000
a-toc	0.8443
asc. acid	0.6468
L2	0.0122
L4	0.0051

CONCLUSION

In the ongoing search for potential therapeutic agents for AD, the Green group aimed to design and produce a new bispyridol containing tetra-aza macrocycle that would primarily target the mis-regulated metal ions and oxidative stress associated with the disease pathology. Thus, **L4** was designed with the hypothesis that by increasing the number of pyridol groups, we could enhance the radical scavenging antioxidant potential of that of **L2**, while still maintaining the metal chelating properties. After successful synthesis and metal-binding studies of **L4** were complete, we evaluated aggregation inhibition and antioxidant activity through a series of assays and other studies. The turbidity assay using tyrosin-10 fluorescence as a marker for aggregation was shown to not be compatible with **L4** due to the solubility effects of pH parameters and metal complexation that occurs. The ability of **L4** to halt redox cycling of Cu(II) in the presence of oxygen and ascorbate was evaluated using the CCA assay, while radical quenching was established using the DPPH radical assay and TEAC assay. The CCA and DPPH studies showed that **L4** could out-perform the parent pyridinophane **L2**, supporting our hypothesis, but the TEAC assay showed both **L2** and **L4** had limited radical scavenging character as compared to Trolox. The results presented here encourage further evaluation of **L4** as a potential AD therapeutic agent. Ongoing and future studies should continue to study these applications as well as the toxicity and metabolic stability of the molecule, especially in cellular model, and any other features of therapeutic agents that contribute to their efficacy and safety.

REFERENCES

1. 2017 Alzheimer's disease facts and figures. *Alzheimer's & Dementia* **2017,** *13* (4), 325-373.

2. 2018 Alzheimer's disease facts and figures. *Alzheimer's & Dementia* **2018,** *14* (3), 367-429.

3. Savelieff, M. G.; Nam, G.; Kang, J.; Lee, H. J.; Lee, M.; Lim, M. H., Development of Multifunctional Molecules as Potential Therapeutic Candidates for Alzheimer's Disease, Parkinson's Disease, and Amyotrophic Lateral Sclerosis in the Last Decade. *Chemical Reviews* **2018,** *119* (2), 1221-1322.

4. Jutkowitz, E.; Kane, R. L.; Gaugler, J. E.; MacLehose, R. F.; Dowd, B.; Kuntz, K. M., Societal and Family Lifetime Cost of Dementia: Implications for Policy. *Journal of the American Geriatrics Society* **2017,** *65* (10), 2169-2175.

5. Buckner, R. L., Memory and executive function in aging and AD: multiple factors that cause decline and reserve factors that compensate. *Neuron* **2004,** *44* (1), 195-208.

6. Sweeney, P.; Park, H.; Baumann, M.; Dunlop, J.; Frydman, J.; Kopito, R.; McCampbell, A.; Leblanc, G.; Venkateswaran, A.; Nurmi, A.; Hodgson, R., Protein misfolding in neurodegenerative diseases: implications and strategies. *Transl Neurodegener* **2017,** *6*, 6.

7. Hardy, J.; Selkoe, D. J., The Amyloid Hypothesis of Alzheimer's Disease: Progress and Problems on the Road to Therapeutics. *Science* **2002,** *297* (5580), 353-356.

8. Jack, C. R.; Knopman, D. S.; Jagust, W. J.; Shaw, L. M.; Aisen, P. S.; Weiner, M. W.; Petersen, R. C.; Trojanowski, J. Q., Hypothetical model of dynamic biomarkers of the Alzheimer's pathological cascade. *The Lancet Neurology* **2010,** *9* (1), 119-128.

9. Josephs, K. A.; Whitwell, J. L.; Ahmed, Z.; Shiung, M. M.; Weigand, S. D.; Knopman, D. S.; Boeve, B. F.; Parisi, J. E.; Petersen, R. C.; Dickson, D. W.; Jack Jr, C. R., β-amyloid burden is not associated with rates of brain atrophy. *Annals of Neurology* **2008,** *63* (2), 204-212.

10. Barnham, K. J.; Bush, A. I., Biological metals and metal-targeting compounds in major neurodegenerative diseases. *Chemical Society Reviews* **2014,** *43* (19), 6727-6749.

11. Bonda, D. J.; Lee, H.-g.; Blair, J. A.; Zhu, X.; Perry, G.; Smith, M. A., Role of metal dyshomeostasis in Alzheimer's disease. *Metallomics* **2011,** *3* (3), 267-270.

12. Kepp, K. P., Bioinorganic Chemistry of Alzheimer's Disease. *Chemical Reviews* **2012,** *112* (10), 5193-5239.

13. Savelieff, M. G.; DeToma, A. S.; Derrick, J. S.; Lim, M. H., The Ongoing Search for Small Molecules to Study Metal-Associated Amyloid-β Species in Alzheimer's Disease. *Accounts of Chemical Research* **2014,** *47* (8), 2475-2482.

14. Francis, P. T.; Palmer, A. M.; Snape, M.; Wilcock, G. K., The cholinergic hypothesis of Alzheimer's disease: a review of progress. *Journal of neurology, neurosurgery, and psychiatry* **1999,** *66* (2), 137-147.

15. Hardy, J. A.; Mann, D. M. A.; Wester, P.; Winblad, B., An integrative hypothesis concerning the pathogenesis and progression of Alzheimer's disease. *Neurobiology of Aging* **1986,** *7* (6), 489-502.

16. Johnston, H. M. Synthesis, characterization, and applications of pyridine- and pyridol-based azamacrocyclic transition metal complexes. Dissertation, TCU, Fort Worth, TX, 2018.

17. Bush, A. I., The metallobiology of Alzheimer's disease. *Trends in Neurosciences* **2003,** *26* (4), 207-214.

18. Lincoln, K. M. Synthesis, Characterization, and Applications of Pyridine- and Pyridol-Based Tetraaza Macrocycles. Dissertation, TCU, Fort Worth, TX, 2015.

19. LaFerla, F. M.; Green, K. N.; Oddo, S., Intracellular amyloid-β in Alzheimer's disease. *Nature Reviews Neuroscience* **2007,** *8*, 499.

20. Lincoln, K. M.; Gonzalez, P.; Richardson, T. E.; Julovich, D. A.; Saunders, R.; Simpkins, J. W.; Green, K. N., A potent antioxidant small molecule aimed at targeting metal-based oxidative stress in neurodegenerative disorders. *Chem Commun (Camb)* **2013,** *49* (26), 2712-4.

21. Burnett, M. E. Understanding the impact of the coordination sphere on metal ions for the design of small molecules in therapeutics and diagnostics. Dissertation, TCU, Fort Worth, TX, 2018.

22. Kozlowski, H.; Luczkowski, M.; Remelli, M.; Valensin, D., Copper, zinc and iron in neurodegenerative diseases (Alzheimer's, Parkinson's and prion diseases) *Coordination Chemistry Reviews* **2012,** *256* (19-20), 2129-2141.

23. Schieber, M.; Chandel, Navdeep S., ROS Function in Redox Signaling and Oxidative Stress. *Current Biology* **2014,** *24* (10), R453-R462.

24. Livingston, G.; Sommerlad, A.; Orgeta, V.; Costafreda, S. G.; Huntley, J.; Ames, D.; Ballard, C.; Banerjee, S.; Burns, A.; Cohen-Mansfield, J.; Cooper, C.; Fox, N.; Gitlin, L. N.; Howard, R.; Kales, H. C.; Larson, E. B.; Ritchie, K.; Rockwood, K.; Sampson, E. L.; Samus, Q.; Schneider, L.

S.; Selbæk, G.; Teri, L.; Mukadam, N., Dementia prevention, intervention, and care. *The Lancet* **2017,** *390* (10113), 2673-2734.

25. Sang, Z.; Wang, K.; Han, X.; Cao, M.; Tan, Z.; Liu, W., Design, Synthesis, and Evaluation of Novel Ferulic Acid Derivatives as Multi-Target-Directed Ligands for the Treatment of Alzheimer's Disease. *ACS Chemical Neuroscience* **2018**.

26. Jones, M. R.; Mathieu, E.; Dyrager, C.; Faissner, S.; Vaillancourt, Z.; Korshavn, K. J.; Lim, M. H.; Ramamoorthy, A.; Wee Yong, V.; Tsutsui, S.; Stys, P. K.; Storr, T., Multi-target-directed phenol–triazole ligands as therapeutic agents for Alzheimer's disease. *Chemical Science* **2017,** *8* (8), 5636-5643.

27. Matheus de Freitas, S.; Kris Simone Tranches, D.; Vanessa Silva, G.; Cindy Juliet Cristancho, O.; Claudio Viegas, J., Multi-Target Directed Drugs as a Modern Approach for Drug Design Towards Alzheimer's Disease: An Update. *Current Medicinal Chemistry* **2018,** *25* (29), 3491-3525.

28. Tarana, U.; Nasimul, H., Alzheimer's Disease: A Systemic Review of Substantial Therapeutic Targets and the Leading Multi-functional Molecules. *Current Topics in Medicinal Chemistry* **2017,** *17* (31), 3370-3389.

29. Lincoln, K. M.; Richardson, T. E.; Rutter, L.; Gonzalez, P.; Simpkins, J. W.; Green, K. N., An N-heterocyclic amine chelate capable of antioxidant capacity and amyloid disaggregation. *ACS Chem Neurosci* **2012,** *3* (11), 919-27.

30. Green, K. N.; Pota, K.; Tircso, G.; Davda, C.; Hyde, K.; Gonzalez, P.; Brewer, S.; Johnston, H. M.; Akkaraju, G., Dialing in on pharmacological features for a therapeutic antioxidant small molecule. *Submitted* **2019**.

31. Johnston, H. M.; Pota, K.; Barnett, M. M.; Kinsinger, O.; Tircsó, G.; Akkaraju, G.; Green, K. N., Enhancement of antioxidant activity and neurotherapeutic features through pyridol addition to tetra-azamacrocyclic molecules. *submitted* **2019**.

32. Alpha, B.; Anklam, E.; Deschenaux, R.; Lehn, J.-M.; Pietraskiewicz, M., 116. Synthesis and Characterization of the Sodium and Lithium Cryptates of Macrobicyclic Ligands Incorporating Pyridine, Bipyridine, and Biisoquinoline Units. *Helv. Chim. Acta* **1988,** *71*, 1042-52.

33. Bottino, F.; Di Grazia, M.; Finocchiaro, P.; Fronczek, F. R.; Mamo, A.; Pappalardo, S., Reaction of Tosylamide Monosodium Salt with Bis(halomethyl) Compounds: An Easy Entry to Symmetrical *N*-Tosyl Aza Macrocycles. *J. Org. Chem.* **1988,** *53*, 3521-9.

34. Pappalardo, S.; Bottino, F.; Di Grazia, M.; Finocchiaro, P.; Mamo, A., A Versatile One-Pot Synthesis of Symmetrical *N*-Tosylazamacrocycles. *Heterocycles* **1985,** *23* (8), 1881-4.

35. Wessel, A. J.; Schultz, J. W.; Tang, F.; Duan, H.; Mirica, L. M., Improved synthesis of symmetrically and asymmetrically *N*-substituted pyridinophane derivatives. *Org. Biolmol. Chem.* **2017,** *15*, 9923-31.

36. Bottino, F.; Di Grazia, M.; Finocchiaro, P.; Fronczek, F. R.; Mamo, A.; Pappalardo, S., Reaction of tosylamide monosodium salt with bis(halomethyl) compounds: an easy entry to symmetrical N-tosyl aza macrocycles. *The Journal of Organic Chemistry* **1988,** *53* (15), 3521-3529.

37. Alonso, E.; Ramón, D. J.; Yus, M., Reductive deprotection of allyl, benzyl and sulfonyl substituted alcohols, amines and amides using a naphthalene-catalysed lithiation. *Tetrahedron* **1997,** *53* (42), 14355-14368.

38. Cody, W. L., Greene's Protective Groups in Organic Synthesis. Fourth Edition. By Peter G. M. Wuts and Theodora W. Greene. John Wiley & Sons, Inc., Hoboken, NJ. 2006. xvii + 1082 pp. 16 × 24 cm. ISBN 0-471-69754-0. $94.95. *Journal of Medicinal Chemistry* **2007,** *50* (5), 1084-1085.

39. Bush, A. I., The metallobiology of Alzheimer's disease. *Trends in Neurosciences* **2003,** *26*, 207-214.

40. Barnham, K. J.; Masters, C. L.; Bush, A. I., Neurodegenerative diseases and oxidative stress. *Nat Rev Drug Discov* **2004,** *3* (3), 205-14.

41. Maynard, C. J.; Bush, A. I.; Masters, C. L.; Cappai, R.; Li, Q. X., Metals and amyloid-beta in Alzheimer's disease. *International Journal of Experimental Pathology* **2005,** *86* (3), 147-159.

42. Miu, A. C.; Benga, O.; Adlard, P. A.; Bush, A. I., Metals and Alzheimer's disease. *J. Alzheimer's Dis.* **2006,** *10* (2,3), 145-163.

43. Rolinski, O. J.; Amaro, M.; Birch, D. J. S., Early detection of amyloid aggregation using intrinsic fluorescence. *Biosens Bioelectron* **2010,** *25* (10), 2249-2252.

44. Amaro, M.; Birch, D. J. S.; Rolinski, O. J., Beta-amyloid oligomerisation monitored by intrinsic tyrosine fluorescence. *Phys Chem Chem Phys* **2011,** *13* (14), 6434-6441.

45. Rolinski, O. J.; Wellbrock, T.; Birch, D. J.; Vyshemirsky, V., Tyrosine Photophysics During the Early Stages of beta-Amyloid Aggregation Leading to Alzheimer's. *The journal of physical chemistry letters* **2015,** *6* (15), 3116-20.

46. Guilloreau, L.; Combalbert, S.; Sournia-Saquet, A.; Mazarguil, H.; Faller, P., Redox Chemistry of Copper–Amyloid-β: The Generation of Hydroxyl Radical in the Presence of

Ascorbate is Linked to Redox-Potentials and Aggregation State. *ChemBioChem* **2007,** *8* (11), 1317-1325.

47. Re, R.; Pellegrini, N.; Proteggente, A.; Pannala, A.; Yang, M.; Rice-Evans, C., Antioxidant activity applying an improved ABTS radical cation decolorization assay. *Free Radical Biology and Medicine* **1999,** *26* (9), 1231-1237.

48. Abramovic, H.; Grobin, B.; Poklar Ulrih, N.; Cigic, B., Relevance and Standardization of In Vitro Antioxidant Assays: ABTS, DPPH, and Folin–Ciocalteu. *Journal of Chemistry* **2018,** *2018*, 9.

49. Csepregi, K.; Neugart, S.; Schreiner, M.; Hideg, E., Comparative Evaluation of Total Antioxidant Capacities of Plant Polyphenols. *Molecules* **2016,** *21* (2).